15th Triennial World Congress, Barcelona, Spain

# NONLINEAR POSITION CONTROL OF A FLEXIBLE BEAM USING SHAPE MEMORY ALLOY ACTUATORS

**M. Moallem**
(mmoallem@engga.uwo.ca)

*Department of Electrical & Computer Engineering*
*The University of Western Ontario*
*London, Ontario, N6G 1H1*
*CANADA*

Abstract: This paper presents a nonlinear control scheme for position control of a flexible beam system using Shape Memory Alloy (SMA) actuators. Due to their interesting properties such as force generation capacity, possibility of miniaturization, and power consumption, these devices have been gaining increased popularity in the past few years. However, SMA actuators possess undesirable characteristics such as nonlinearities, hysteresis, extreme temperature dependencies, and slow response that make them difficult to use in precision applications. By taking into account the nonlinear and thermal characteristics, a control scheme is developed in order to regulate the force exerted by an SMA actuator attached to a flexible beam. The control scheme is based on input-output linearization of the nonlinear system. The control goal is to regulate the force exerted by the SMA actuator to a desired value. The internal dynamics of the system is derived and it is shown that these dynamics can be stabilized by proper choice of controller gain matrices. Simulation results are presented based on the data for a setup that is currently under construction in our laboratory.

Keywords: Output feedback, position control, nonlinear systems, flexible arm, actuators, vibration dampers.

## 1. INTRODUCTION

Smart material systems offer great possibilities in terms of providing novel and economical solutions to engineering problems. The technological advantages of these materials over traditional ones are due to their unique microstructure and molecular properties. Smart materials such as piezo-electric transducers (PZT), shape memory alloys (SMA), magneto- and electro-rheological fluids (MRF and ERF), and fiber-optic sensors have been used in such diverse areas areas as automotive vehicles, robots, orthodontic treatment, biotechnology, civil engineering structures, space structures, sports equipment, etc. (see e.g., (Janocha 1999), (Otsuka and Wayman 1998)).

In this regard, shape memory alloys possess an interesting property by which the metal *remembers* its original shape and reverts to it at a characteristic transformation temperature. Although this property was first observed in 1932 for gold-cadmium alloys, it was not until 1962 that such properties were discovered for nickel-titanium alloys (Srinivasan and McFarland 2001). The last decade of the twentieth century witnessed a dramatic growth in the applications of SMA materials made from nickel-titanium (NiTi) alloys. Hashimoto *et al.* (1985) used SMA wires to provide lightweight actuation for walking robots. Grant and Hayward (1997) proposed a novel shape memory alloy actuator with improved accuracy and speed. Madhil and Wang (1988) studied the hysteresis and nonlinear characteristics of an SMA actuator for a position control system which was used to prove its *L2*-stability. The SMA actuators have been used for vibration control of flexible beams, see e.g., (Baz, Imam and McCoy 1990), (Choi, Park and Fukuda 1988), (Choi and Cheong 1996).

However, these works have not taken into account the nonlinear effects of SMA actuators and the effect of temperature on performance of the vibration control scheme. In this paper we follow a different scheme for achieving precise position control. The approach is to regulate the force exerted by the SMA actuator on a flexible cantilevered beam to reach a value that corresponds to a desired position of the beam. It is shown that small errors can be achieved by proper choice of feedback gains while the internal dynamics remain stable. Simulation results are given for a setup that is currently under development in our laboratory.

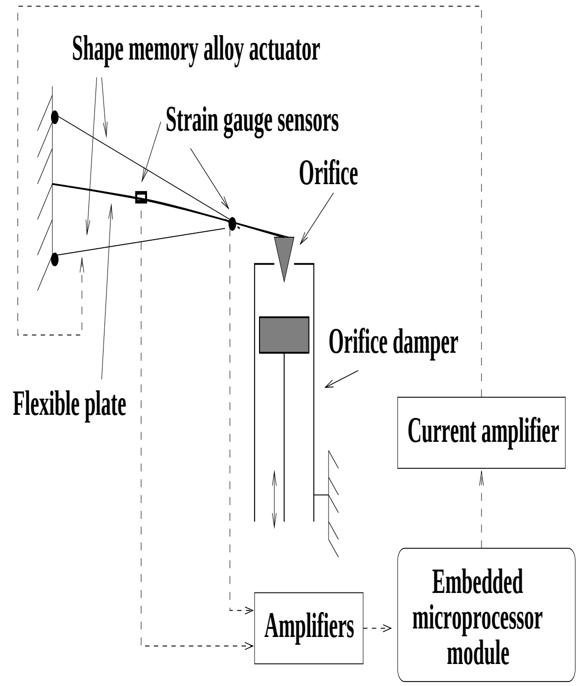


Figure 1: Smart damper using an SMA actuator.

## 2. SYSTEM MODELING AND CONTROL

There are several applications where one may be concerned with controlling the end-point position of a flexible beam. The motivation for the present work is stemmed from an application as depicted in Figure . An embedded module consisting of a small microprocessor system is utilized to continuously adjust the diameter of an orifice such that a desired damping coefficient is achieved. A good candidate for adjusting the orifice is by means of two SMA wire actuators. When no current is passing through the SMA strings, the orifice is open with maximum diameter. By passing an electric current through one of the SMA strings the beam can be bent to change the orifice diameter. Only one of the two SMA wires is actuated at any time depending on the desired direction of motion. This is to speed up the response of the system since the heating time constant is larger than the cooling time constant. The goal is to place the tip position at a desired location in the presence of disturbance forces resulting from air flowing through the orifice and acting at the end-point of the flexible beam. Taking into account the non-linearity and the temperature dependence of the SMA wire, the dynamics of the system is given by

$$M\ddot{\delta} + K\delta = bn(T) \quad (1)$$

$$\dot{T} + \beta T = \alpha u \quad (2)$$

where $\delta$ is the $n \times 1$ vector of flexible modes, $M$ and $K$ are the $n \times n$ mass and stiffness matrices of the flexible beam, respectively, obtained using the Lagrangian formulation (see e.g., (Meirovitch 1975) ), $b$ is the input-effect vector, $n(T)$ is the temperature dependent nonlinear force generated by the SMA wire, $T$ is the wire temperature, and $\alpha$, $\beta$ are positive constants. Equation (2) is obtained from the heat transfer dynamics of a single wire expressed as (Madhil and Wang 1988)

$$\rho c V \frac{dT}{dt} = Ri^2(t) - hA(T - T_a) \quad (3)$$

where $\rho$ $(kg/m^3)$ is the mass density of wire material, $c$ $(Jkg^{-1}{}^\circ C^{-1})$ is the specific heat, $V$ $(m^3)$ is the volume of wire, $i$ $(A)$ is the electric current, $R$ $(\Omega)$ is the wire resistance, $h$ $(Wm^{-2}{}^\circ C^{-1})$ is the convection heat transfer coefficient, $A$ $(m^2)$ is the surface area of the wire, and $T_a$ is the ambient temperature. Note that the input $u$ in (2) can take positive and negative values that correspond to the inputs applied to the two wires in Figure .

Considering the dynamics in (1)–(2), let us define the output as

$$y_o = \Psi \delta \quad (4)$$

where $\Psi$ is a constant matrix that relates modal variables to the output of interest $y_o$, which can be the displacement of the tip position of the beam or a location close to the tip. Taking the time derivative of $y_o$ twice and using (1) we have

$$\ddot{y}_o = \Psi M^{-1}(bn_o(T) - K\delta) \quad (5)$$

where $n_o(T)$ is the desired $n(T)$ corresponding to $y_o$. Let us further take $n_o(T)$ according to

$$n_o(T) = (\Psi M^{-1} b)^{-1}(v + \Psi M^{-1} K\delta) \quad (6)$$

where $v$ is a new input. Substituting the above equation in (5) yields

$$\ddot{y}_o = v \tag{7}$$

Denoting the reference position by $y_r$ and the error by $e = y_r - y_o$, let us choose $v$ as

$$v = -K_d \dot{y}_o + K_p e \tag{8}$$

where $K_d$ and $K_p$ are feedback gains and it is assumed that $\dot{y}_o$ is known by measurement or estimation. The resulting closed-loop system will then be given by

$$\ddot{e} + K_d \dot{e} + K_p e = 0 \tag{9}$$

Now substituting (8) in (6) yields

$$\begin{aligned} n_o(T) &= \frac{1}{\Psi M^{-1} b}(K_p e + K_d \dot{e} \\ &+ \Psi M^{-1} b K \delta) \end{aligned} \tag{10}$$

A main goal of the controller is to make $n(T)$ approach $n_o(T)$. Thus let us define the output to be controlled as

$$\begin{aligned} y &= n(T) - n_o(T) = n(T) - \frac{1}{\Psi M^{-1} b} \\ &\times (K_p e + K_d \dot{e} + \Psi M^{-1} b K \delta) \end{aligned} \tag{11}$$

Following the input-output linearization method (Slotine and Li 1991), only one time derivative of y is required so that the input $u$ appears in the equations, which after some algebraic manipulations yields

$$\begin{aligned} \dot{y} &= \frac{\partial n}{\partial T}(-\beta T + \alpha u) + K_d n(T) \\ &- \frac{K_d \Psi M^{-1} K}{\Psi M^{-1} b}\delta + \frac{K_p \Psi - \Psi M^{-1} K}{\Psi M^{-1} b}\dot{\delta} \end{aligned} \tag{12}$$

The above equation describes part of the dynamics of the system that is related to the input-output behavior. The other part of the dynamics, often referred to as *internal dynamics* (Slotine and Li 1991), can be obtained by solving for $n(T)$ in (11), i.e.,

$$\begin{aligned} n(T) &= y + \frac{1}{\Psi M^{-1} b}(K_p e + K_d \dot{e} \\ &+ \Psi M^{-1} b K \delta) \end{aligned} \tag{13}$$

and substituting (13) in (1), which yields the internal dynamics given by

$$\begin{aligned} \ddot{\delta} &= -M^{-1}((I - \frac{b \Psi M^{-1}}{\Psi M^{-1} b})K \\ &+ K_p \frac{b \Psi}{\Psi M^{-1} b})\delta - K_d \frac{M^{-1} b \Psi}{\Psi M^{-1} b}\dot{\delta} \\ &+ M^{-1} b \left(y + K_p \frac{y_r}{\Psi M^{-1} b}\right). \end{aligned} \tag{14}$$

It can be concluded from (14) that the internal dynamics can be stabilized by a proper choice of feedback gains $K_p$ and $K_d$, provided that the internal dynamics are controllable. This is usually the case as can be verified for a model with a single mode (scalar $\delta$) which is the most important mode to control.

Now let us write (14) in the form

$$\dot{\Delta} = A_\Delta \Delta + b_\Delta (y + \frac{K_p y_r}{\Psi M^{-1} b}) \tag{15}$$

where

$$\begin{aligned} A_\Delta &= \begin{bmatrix} 0 & I \\ A_{21} & -K_d \frac{M^{-1} b \Psi}{\Psi M^{-1} b} \end{bmatrix} \\ \Delta &= [\delta^T \quad \dot{\delta}^T], \; b_\Delta = \begin{bmatrix} 0 \\ M^{-1} b \end{bmatrix} \end{aligned} \tag{16}$$

with

$$\begin{aligned} A_{21} &= -M^{-1}((I - \frac{b \Psi M^{-1}}{\Psi M^{-1} b})K \\ &+ K_p \frac{b \Psi}{\Psi M^{-1} b}). \end{aligned} \tag{17}$$

Furthermore, (12) can be written as

$$\dot{y} = h_1 u + h_2 + h_3 \tag{18}$$

where

$$\begin{aligned} h_1 &= \alpha \frac{\partial n}{\partial T} \\ h_2 &= K_d n(T) - \frac{K_d \Psi M^{-1} K}{\Psi M^{-1} b}\delta \\ &+ \frac{K_p \Psi - \Psi M^{-1} K}{\Psi M^{-1} b}\dot{\delta} \\ h_3 &= -\beta \frac{\partial n}{\partial T} T. \end{aligned} \tag{19}$$

Of the above terms, $h_1$ is of known sign and approximate value, $h_2$ is completely known, and the sign of $h_3$ is known but its value is not available since its is assumed that the wire temperature $T$ is not measured. Let us choose the control law as

$$u = \hat{h}_1^{-1}\left(-k_y s(k_s y) - h_2\right) \tag{20}$$

where $\hat{h}_1$ is an estimate of $h_1$, and $s(\cdot)$ is a *smooth* nonlinear saturating function (e.g., $tanh(\cdot)$) that approximates a $sign(\cdot)$ function. This control law is obtained by following a sliding control approach as follows (Slotine and Li 1991) . Let $\sigma = y$ and consider a switching surface $\sigma = 0$. The sliding condition can be ensured if $\sigma \dot{\sigma} \leq -k_\sigma |\sigma|$ for some positive constant $k_\sigma$. Using the control law given by (20), with $s(\cdot)$ replaced by $sign(\cdot)$, we have

$$\begin{aligned} \sigma \dot{\sigma} &= -k_y h_1 \hat{h}_1^{-1} y (sign(y) \\ &- \frac{((1 - h_1 \hat{h}_1^{-1}) h_2 + h_3)}{k_y h_1 \hat{h}_1^{-1}}) \end{aligned} \tag{21}$$

It can be concluded from (21) that for a bounded region $C \subset R^{2n+1}$ in the state-space of $(\Delta, T)$, the sliding condition can be ensured by selecting $k_y$ large enough. This is due to the boundedness of $h_1$, $h_2$, and

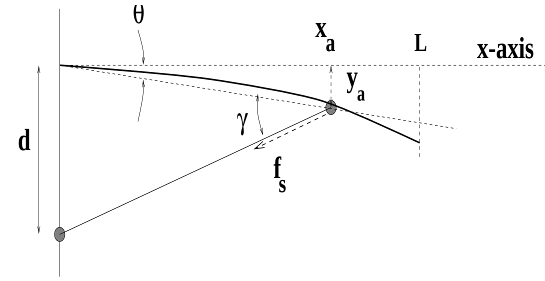


Figure 2: SMA actuator.

$h_3$, and the effect of $k_y$ in the denominator in (21). Depending on the sign of $y$, the term in parenthesis can be made positive or negative by selecting $k_y$ large enough.

The control law in (20) is a modification of the sliding control law to reduce undesirable effects such as control chattering. In order to show the stability of the whole system let us choose a Lyapunov function candidate given by

$$V = \frac{1}{2}y^2 + \epsilon_\Delta^2 \Delta^T P_\Delta \Delta \tag{22}$$

where $\epsilon_\Delta^2$ is a small scaling constant. The scaling constant is introduced as a result of the stability requirement that $y$ converges to a small value near zero while $\Delta$ remains bounded. A proof of the closed-loop system stability can be established based on the Lyapunov function candidate (22) and the system dynamics given by (12), (14). The reader is referred to (Moallem *et al.* 1998), (Moallem *et al.* 2000) for a similar analysis.

## 3. KINEMATIC RELATIONSHIPS

The input effect vector $b$ in (1) depends on the place where the SMA wires are attached. In order to obtain this vector refer to Figure , which is comprised of a cantilevered flexible beam attached to SMA wires one of which is shown in figure. Let $f_s$ be the force exerted by the SMA string which is placed at $x_a$ along the link. It is assumed that this force is measurable using a sensor mounted on the flexible link or at the other end of the string. Then neglecting the curvature of the beam, the tangential and normal components of $f_s$, denoted by $f_{sT}$ and $f_{sN}$, are obtained as

$$f_{sT} = f_s cos(\gamma), \quad f_{sN} = f_s sin(\gamma). \tag{23}$$

The angle $\gamma$ can be obtained from

$$\gamma = tan^{-1}\left(\frac{d - y_a cos(\theta/2)}{x_a cos(\theta)}\right) + \theta \tag{24}$$

with $y_a$ is given by

$$y_a = \sum_{i=1}^{n} \phi_i(x_a)\delta_i \tag{25}$$

where $\phi_i(x_a)$ is mode $i$'s shape function. Using the method of virtual work and the Lagrangian formulation (see e.g. (Meirovitch 1975)) one can obtain the input effect vector $b$ with element its element $i$ given by

$$b_i = f_s sin(\gamma)\phi_i(x_a) \tag{26}$$

Assuming that $\theta$ is small enough and $d \gg y_a$ we have

$$b_i = \frac{d}{\sqrt{d^2 + x_a^2}}\phi_i(x_a) \tag{27}$$

## 4. NUMERICAL SIMULATIONS

The control scheme developed in the previous section was simulated for the system shown in Figure  with the following numerical values:

$$\begin{aligned} L &= 0.4m, \quad x_a = 0.3m, \quad d = 0.4m, \\ K_d &= 8, \quad K_p = 16, \quad k_y = 10, \\ k_s &= 100000, \quad \beta = 0.5, \quad \alpha = 0.6, \\ T_a &= 25°C, \\ M &= diag([0.1832,\ 0.1639]), \\ K &= diag([79.3,\ 4029.5]). \end{aligned} \tag{28}$$

The model was obtained using the method of assumed modes (Meirovitch 1975)) for a steel plate of dimensions $0.5mm \times 0.2m \times 0.4m$ that is attached to two SMA wires made of $NiTi$. Figure  shows simulation results when the nonlinear function $n(T)$ in (1) is chosen as $n(T) = 20\, tanh(0.1(T - T_a))$. The nonlinear input in (20) was chosen as $u = 5(-10\, tanh(100000y) - h_2)$, i.e., $\hat{h}_1^{-1} = 5$, $k_y = 10$, $k_s = 100000$. From (19), it follows that $h_1 = 1$ for $T_a = 25°C$, which differs from $\hat{h}_1$ by a factor of five. The results indicate that good regulation of tip deflection can be achieved despite these uncertainties.

## 5. CONCLUSION

In this paper a nonlinear control scheme was developed for position control of a flexible beam actuated by Shape Memory Alloy wires. SMA actuators exhibit highly nonlinear effects with characteristics that are highly temperature dependent. Since actuator temperature is not readily measurable, it is treated as a disturbance term that has to be compensated by the control scheme. By following an approach similar to sliding-mode control, a control scheme was developed to regulate the force exerted by the actuator on the flexible beam. The flexible beam has a rather deterministic model. Hence the reference force is obtained to achieve a desirable position of the beam end-point. The control scheme does not suffer from the chattering phenomena associated with sliding-mode control while providing a small regulation error that may be

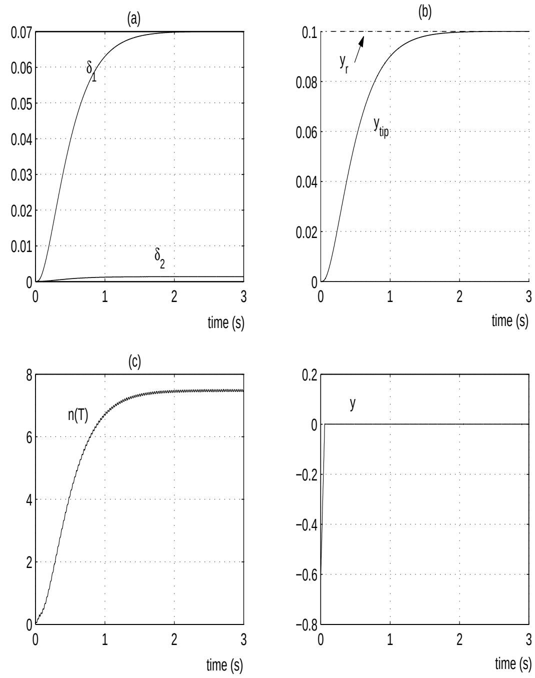


Figure 3: Simulation results: (a) Modal variables ($m$), (b) Tip deflection and reference position ($m$), (c) Force exerted by SMA actuator ($N$), (d) Error between desired and actual forces exerted by SMA,. i.e., output y ($N$).

acceptable in practical applications. The experimental phase of this project is currently under way in our research laboratory.

## 6. ACKNOWLEDGEMENTS

This research was supported in part by the Natural Sciences and Engineering Research Council of Canada (NSERC) and by the University of Western Ontario Academic Development Fund.

## REFERENCES


Baz, A. Imam, K. and McCoy, J.: 1990, Active vibration control of flexible beams using shape memory actuators, *Journal of Sound and Vibration* **140**, 437-456.

Choi, S. B., Park, Y. and Fukida, T.: 1998, A proof-of-concept investigation on active vibration control of hybrid smart structures, *Mechatronics* **8**, 673-689.

Choi, S. and Chong, C. C.: 1996, Vibration control of a flexible beam using shape memory alloy actuators, *Journal of Guidance, Control, and Dynamics* **19**, 1178-1180.

Grant, D. and Hayward, V.: 1997, Variable structure control of shape memory alloy actuators, *IEEE Control Systems Magazine* **17**, 80-88.

Hashimoto, M., Takeda, M., Sagawa, H., Chiba, I. and Sat, K.: 1985, Shape memory alloy and robotic actuators, *Journal of Robotic Systems* **2**, 3-25.

Janocha, H.: 1999, *Adaptronics and Smart Structures: Basics, Materials, Design, and Applications*, Springer-Verlag, Berlin.

Madhill, D. and Wang, D.: 1998, Modeling and l2–stability of a shape memory alloy position control system, *IEEE Transactions on Control System Technology* **6**, 473-481.

Meirovitch, L.: 1975, *Elements of Vibration Analysis*, McGraw–Hill, New-York.

Moallem, M., Khorasani, K. and Patel, R.: 1998, Inversion–based sliding control of a flexible–link manipulator, *International Journal of Control* **71**, 477-490.

Moallem, M., Patel, R. and Khorasani, K.: 2000, *Flexible-Link Robot Manipulators: Control Techniques and Structural Design*, London.

Otsuka, K. and Wayman, C.: 1998, *Shape Memory Materials*, Cambridge University Press, Cambridge, UK.

Slotine, J.-J. E. and Li, W.: 1991, *Applied Nonlinear Control*, Prentice–Hall, Englewood Cliffs, NJ.

Srinivasan, A. and McFarland, D.: 2001, *Smart Structure Analysis and Design*, Cambridge University Press, Cambridge, UK.